Journal of Computational Mathematics
Vol.31, No.5, 2013, 532–548.

http://www.global-sci.org/jcm
doi:10.4208/jcm.1307-m4290

A LOCAL MULTILEVEL PRECONDITIONER FOR THE ADAPTIVE MORTAR FINITE ELEMENT METHOD*

Feng Wang Jinru Chen
Jiangsu Key Laboratory for NSLSCS, School of Mathematical Sciences, Nanjing Normal University, Nanjing 210023, China
Email: fwang@njnu.edu.cn jrchen@njnu.edu.cn

Abstract

In this paper, we propose a local multilevel preconditioner for the mortar finite element approximations of the elliptic problems. With some mesh assumptions on the interface, we prove that the condition number of the preconditioned systems is independent of the large jump of the coefficients but depends on the mesh levels around the cross points. Some numerical experiments are presented to confirm our theoretical results.

Mathematics subject classification: 65N30, 65N55, 65F10.
Key words: Mortar, Adaptive finite element method, Local multilevel method, Additive Schwarz method.

1. Introduction

In this paper, we present a local multilevel preconditioner for the adaptive mortar finite element method for the following second order elliptic problems:

$$\begin{cases} -\nabla \cdot (\rho \nabla u) = f, & \text{in } \Omega, \\ u = 0, & \text{on } \partial\Omega, \end{cases} \tag{1.1}$$

where $\rho > 0$ is a piecewise constant, $f \in L^2(\Omega)$, and Ω is a polygonal domain.

The mortar finite element method is a technique for dealing with different discretization schemes on different subdomains [1, 2]. It is effective for solving problems with complicated geometries, heterogeneous material, multi-physics, and so on. In this paper, we use the mortar finite element method to handle the nonmatching meshes. Based on a posteriori error estimators, the adaptive finite element methods are now widely used to achieve better accuracy with minimum degrees of freedom. Combining the mortar approach and the adaptive finite element methods, many researchers propose different a posteriori error estimators (see [7, 8] and the references therein for details). The first author and his collaborator [23] also proposed some residual-based a posteriori error estimators, and the analysis does not require saturation assumptions or mesh restrictions on the interface which are often needed in the literature. However, there are rather few results on developing efficient solvers for the discrete problems. Based on quasi-uniform grids, Wohlmuth [26] and Gopalakrishnan [17] introduced V-cycle and W-cycle multigrid methods for the mortar finite element method for elliptic problems respectively. Xu and Chen [31] discussed a W-cycle multigrid algorithm for the mortar element method for the P_1 nonconforming element.

* Received October 12, 2012 / Revised version received April 12, 2013 / Accepted July 9, 2013 / Published online August 27, 2013 /

Since the mesh is refined locally in the process of adaptivity, traditional multigrid methods, in which the smoothing is performed on all nodes, may not be optimal or quasi-optimal (see [19]). Wu and Chen [27] first proved that the local multigrid method, in which the smoothing was performed on new nodes and their "immediate" neighbors of each level, was optimal for the adaptive finite element method for the Poisson equation in two dimension. In [13, 15], Xu, etc., introduced and analyzed some local multigrid methods based on reconstructed adaptive grid, which was applied to the adaptive finite element methods for the elliptic problems with discontinuous coefficients [14]. Based on the adaptive grid, Xu and Chen [11, 12, 30] also proposed and analyzed some local multilevel methods for P_1 conforming and nonconforming element methods for the elliptic problems. Recently, Lu, Shi and Xu [18] considered the local multilevel methods for discontinuous Galerkin finite element method on adaptively refined meshes.

The purpose of this paper is to present a local multilevel preconditioner for the mortar finite element method for the second order elliptic problems with discontinuous coefficients. Since the finite element spaces are nonnested, intergrid transfer operators, which are stable under the weighted L^2 norm and energy norm, are introduced to exchange information between different meshes. On each level, the smoothing is performed on the new free nodes and the old free nodes associated with which the basis functions are changed. In addition, we also need to smooth on all the mortar side nodes on the finest level. With the assumption that each mortar side edge is the union of some whole nonmortar side edges (see Fig. 2.2 for an illustration), we prove that the condition number of preconditioned system is independent of the large jump of the coefficients but relies logarithmically on the mesh size around the cross points.

The remainder of the paper is organized as follows. In Section 2, we present the discrete problem and some notations. The local multilevel preconditioner is proposed in Section 3. In Section 4, we give the condition number estimate of the preconditioned system. Finally, we present some numerical experiments to confirm our theoretical results.

For convenience of discussions, we usually use inequalities $a \lesssim b$, $a \simeq b$ to replace $a \leq Cb$ and $cb \leq a \leq Cb$ with some multiplicative mesh size and coefficient independent constants $c, C > 0$ that depend only on the domain Ω and the shape (e.g., through the aspect ratio) of elements.

2. Preliminary

The weak form of the problem (1.1) is to find $u \in H_0^1(\Omega)$ satisfying

$$a(u, v) \triangleq (\rho \nabla u, \nabla v) = (f, v), \quad \forall v \in H_0^1(\Omega). \tag{2.1}$$

Let Ω be partitioned into non-overlapping polygonal subdomains $\{\Omega_i\}_{i=1}^N$. We only consider the geometrically conforming case, i.e., the intersection between the closure of two different subdomains is empty, a vertex, or an edge. The coefficient ρ is a constant when restricted to each subdomain Ω_i. We use Γ_{ij} to denote the common open edge of Ω_i and Ω_j, $\Gamma = \bigcup_{ij} \Gamma_{ij}$. Given an initial shape regular triangulation $\mathcal{T}_1(\Omega)$, which is conforming in each subdomain, $\{\mathcal{T}_l(\Omega), 2 \leq l \leq L\}$ is a set of triangulations generated by the adaptive finite element procedure [23]. We note that the resulting triangulation $\mathcal{T}_l(\Omega)$ can be non-matched across adjacent subdomain interfaces, so each Γ_{ij} can be regarded as two sides corresponding to the two subdomains Ω_i and Ω_j. We call one of the sides of Γ_{ij} as the mortar side and the other one as the nonmortar side. For each interface, we choose the side of the subdomain on which the coefficient is larger

as the mortar side, and the other side as the nonmortar side. If there is no jump in the coefficient across the interface, the choice is arbitrary. This can always be done in practice for the geometrically conforming domain decomposition.

For each Γ_{ij}, we usually denote the mortar and nonmortar sides of Γ_{ij} by $\gamma_{m(i)}$ and $\delta_{m(j)}$ respectively. Here the subscript m represents the index of Γ_{ij}, and the subscripts i, j indicate that the mortar and nonmortar sides are parts of boundaries of Ω_i and Ω_j respectively. The two sets $\mathcal{T}_l(\gamma_{m(i)})$ and $\mathcal{T}_l(\delta_{m(j)})$ are the $1D$ triangulations inherited from $\mathcal{T}_l(\Omega_i)$ and $\mathcal{T}_l(\Omega_j)$ respectively (see Fig. 2.1), where $\mathcal{T}_l(\Omega_i)$ and $\mathcal{T}_l(\Omega_j)$ are the restrictions of $\mathcal{T}_l(\Omega)$ to Ω_i and Ω_j. We use γ and δ to denote the mortar and nonmortar sides of Γ, i.e.,

$$\gamma = \cup_m \gamma_{m(i)}, \quad \delta = \cup_m \delta_{m(j)}.$$

Accordingly, $\mathcal{T}_l(\gamma) = \cup_m \mathcal{T}_l(\gamma_{m(i)})$ and $\mathcal{T}_l(\delta) = \cup_m \mathcal{T}_l(\delta_{m(j)})$ are the sets of edges of the lth level mesh on mortar and nonmortar sides respectively.

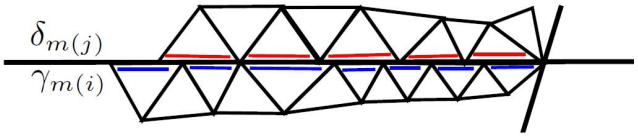

Fig. 2.1. An illustration of the set $\mathcal{T}_l(\delta_{m(j)})$ and $\mathcal{T}_l(\gamma_{m(i)})$.

For any geometry element G, $\mathcal{N}_l(G)$ denotes the set of nodes in G of the triangulation $\mathcal{T}_l(\Omega)$, and $\mathcal{N}_l(\overline{G})$ denotes the set of corresponding nodes in $\overline{G}$. Specially, we use $\mathcal{N}_l(\Omega)$ to denote the set of the nodes of $\mathcal{T}_l(\Omega)$ which are in Ω but not on the interface. The notation h_G indicates the diameter of G, and ρ_G denotes the restriction of ρ to G.

Let $X_l(\Omega_i)$ be the P_1 conforming element space defined on $\mathcal{T}_l(\Omega_i)$, $X_l(\Omega) = \prod_{i=1}^N X_l(\Omega_i)$. For each nonmortar side $\delta_{m(j)}$, $M_l(\delta_{m(j)}) = \text{span}\{\psi^k_{m(j)}\}$ denotes the dual Lagrange multiplier space defined on $\mathcal{T}_l(\delta_{m(j)})$, where $\psi^k_{m(j)}$ is the dual function associated with the interior node p_k of $\mathcal{T}_l(\delta_{m(j)})$ and satisfying (see [25])

$$\int_{\delta_{m(j)}} \psi^k_{m(j)} \phi^s_{m(j)}|_{\delta_{m(j)}} d\sigma = \begin{cases} \int_{\delta_{m(j)}} \phi^k_{m(j)}|_{\delta_{m(j)}} d\sigma, & \text{if } k = s, \\ 0, & \text{otherwise}, \end{cases} \tag{2.2}$$

with $\phi^s_{m(j)} \in X_l(\Omega)$ the basis function associated with the node p_s.

Next, we introduce the mortar finite element space on $\mathcal{T}_l(\Omega)$ as follows:

$$V_l = \Big\{ v \in X_l(\Omega) : \big(v|_{\gamma_{m(i)}} - v|_{\delta_{m(j)}}\big) \in H^{\frac{1}{2}}_{00}(\Gamma_{ij}), \quad \int_{\delta_{m(j)}} (v|_{\gamma_{m(i)}} - v|_{\delta_{m(j)}}) \psi d\sigma = 0,$$
$$\forall \gamma_{m(i)} = \delta_{m(j)} = \Gamma_{ij}, \quad \psi \in M_l(\delta_{m(j)}) \Big\}. \tag{2.3}$$

Here $\cdot|_{\gamma_{m(i)}}$ and $\cdot|_{\delta_{m(j)}}$ denote the restrictions from the mortar side and nonmortar side subdomains Ω_i and Ω_j to the interface respectively, and we will omit them if there is no confusion. The condition in (2.3) for each interface is called *mortar condition*, through which the basis functions in V_l are associated with the nodes in $\widetilde{\mathcal{N}}_l = \mathcal{N}_l(\Omega) \cup \mathcal{N}_l(\gamma) \cup \mathcal{C}$, where $\mathcal{C}$ is set of cross points. We call these nodes in $\widetilde{\mathcal{N}}_l$ as free nodes.

The mortar finite element approximation to the original problem (2.1) is to find $u_L \in V_L$ such that

$$a_L(u_L, v_L) = (f, v_L), \quad \forall\, v_L \in V_L, \tag{2.4a}$$

where

$$a_L(u_L, v_L) = \sum_{i=1}^{N} \int_{\Omega_i} \rho \nabla u_L \cdot \nabla v_L dx. \tag{2.4b}$$

By the definition, the bilinear form $a_L(\cdot,\cdot)$ is also well-defined on the space V_l, and we denote it by $a_l(\cdot,\cdot)$ with the corresponding norm $\|\cdot\|_{a_l} = \sqrt{a_l(\cdot,\cdot)}$. We use $(\cdot,\cdot)_{0,\rho,G}$ to denote the weighted L^2 inner product on G, i.e., $(\cdot,\cdot)_{0,\rho,G} = (\rho\cdot,\cdot)_{L^2(G)}$, $\|\cdot\|_{0,\rho,G}$ is the induced norm. We usually omit the subscript when $G = \Omega$.

In this paper, we assume that each edge element on the mortar side is the union of a number of whole elements on the nonmortar side (see Fig. 2.2 for an illustration). Consequently, V_l includes a conforming finite element subspace $W_l \triangleq V_l \cap H_0^1(\Omega)$, which is the space defined on the triangulation with hanging nodes (see [9] for example). For each mortar side edge $e \in \mathcal{T}_l(\gamma)$, N_l^e denotes the number of corresponding nonmortar side edges, and $J_e^\rho = \rho_{\Omega_i}/\rho_{\Omega_j}$ indicates the rate of coefficients on mortar and nonmortar side subdomains Ω_i and Ω_j associated with e. It is known by the rule choosing the mortar side that $J_e^\rho \geq 1$.

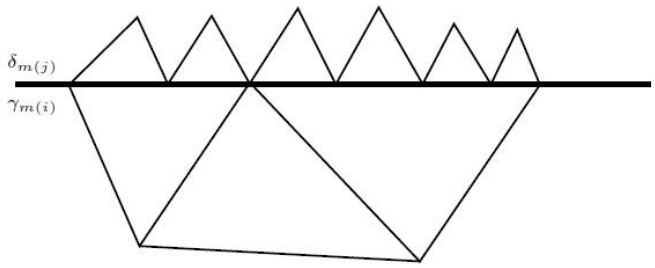

Fig. 2.2. An illustration of the mesh on the mortar and nonmortar sides.

Remark 2.1. We note that the constraint $\left(v|_{\gamma_{m(i)}} - v|_{\delta_{m(j)}}\right) \in H_{00}^{1/2}(\Gamma_{ij})$ in (2.3) is to ensure that the functions in V_l are continuous at the cross points. Therefore, we do not need treating the cross points specially when designing intergrid transfer operators. If the constraint is omitted, since the finite element function is discontinuous at the cross points, we should carefully choose suitable prolongation operator which is stable under the weighted L^2 norm and the energy norm.

3. The Local Multilevel Preconditioner

In this section, we shall propose our local multilevel preconditioner.

We first introduce a transfer operator from V_{l-1} to V_L. Since $X_{l-1}(\Omega_i) \subset X_l(\Omega_i)$, let $I_{l-1}^i : X_{l-1}(\Omega_i) \to X_l(\Omega_i)$ be the natural prolongation operator. Then for any $v \in V_{l-1}$, we define $I_{l-1}v \in W_l \subset V_l$ by its nodal values. For the non-interface node $p \in \mathcal{N}_l(\Omega_i) \cup \mathcal{N}_l(\partial\Omega) \cup \mathcal{C}$, let

$$\left(I_{l-1}v\right)(p) = v(p), \tag{3.1}$$

while for the interface node $p \in \mathcal{N}_l(\gamma_{m(i)}) \cup \mathcal{N}_l(\delta_{m(j)})$ (see Fig. 3.1), we take the corresponding mortar side nodal value, i.e.,

$$\left(I_{l-1}v\right)(p) = \left(I_{l-1}^i v\right)(p). \tag{3.2}$$

By the mesh assumption on the mortar and nonmortar sides and the fact that $I_{l-1}^i v$ is piecewise linear and continuous on Γ_{ij}, the definition (3.2) ensures that $I_{l-1}v$ is continuous across the

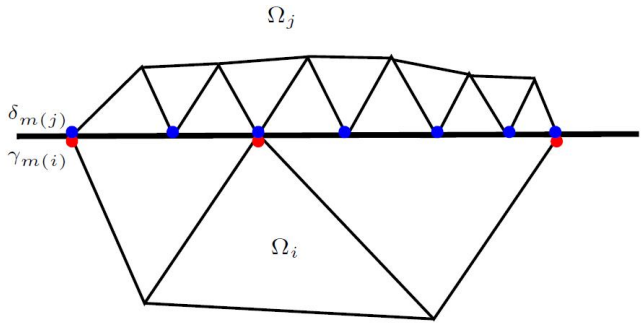

Fig. 3.1. Nodes on mortar and nonmortar sides

interface. Obviously, $I_{l-1}u$ is a function in V_l. Due to $W_l \subset W_L \subset V_L$, it is also a function in the finest space V_L. Thus the operator I_{l-1} defines an extension from V_{l-1} to V_L.

Next, we will define the set of the nodes of $\mathcal{T}_l(\Omega)$, $2 \le l \le L$, on which local smoothers are carried out. Let $\mathcal{S}_l$ be the set of new free nodes of $\mathcal{T}_l(\Omega)$ and the nodes associated with which the basis functions are modified, i.e.,

$$\mathcal{S}_l = \left\{ p : p \in \widetilde{\mathcal{N}}_l \setminus \widetilde{\mathcal{N}}_{l-1} \text{ or } p \in \widetilde{\mathcal{N}}_l \cap \widetilde{\mathcal{N}}_{l-1} \text{ satisfying } \widetilde{\phi}_l^p \neq \widetilde{\phi}_{l-1}^p \right\},$$

where $\widetilde{\phi}_l^p \in V_l$, $\widetilde{\phi}_{l-1}^p \in V_{l-1}$ are the basis functions corresponding to the node p. On the finest level, the set $\mathcal{S}_L$ is enlarged to include all the mortar side nodes, i.e., $\mathcal{S}_L := \mathcal{S}_L \cup \mathcal{N}_L(\gamma)$. We denote $\widetilde{V}_l \subset V_l$ the space spanned by the basis functions associated with the nodes in $\mathcal{S}_l$, i.e., $\widetilde{V}_l = \text{span}\{\widetilde{\phi}_l^p, p \in \mathcal{S}_l\}$. Correspondingly, V_L admits a decomposition (see (4.17))

$$V_L = I_1 V_1 + \sum_{l=2}^{L} I_l \widetilde{V}_l, \tag{3.3}$$

where I_L is the identical operator. We also denote $\widetilde{V}_1 = V_1$ for convenience.

On each subspace $\widetilde{V}_l, 2 \le l \le L$, let $R_l : \widetilde{V}_l \to \widetilde{V}_l$ be a symmetric positive definite smoothing operator. We assume that R_l satisfies the following equivalence

$$(R_l^{-1} v, v)_{0,\rho} \simeq (h_l^{-2} v, v)_{0,\rho}, \quad \forall v \in \widetilde{V}_l, \tag{3.4}$$

where h_l^{-1} is a piecewise constant defined by the reciprocal of the diameters of the elements in $\mathcal{T}_l(\Omega)$. On the coarsest level, we use the exact solver, i.e., $R_1 = A_1^{-1}$. Here A_1 is the operator satisfying $(A_1 w, v) = a_1(w, v)$ for any w, v in V_1.

Remark 3.1. The standard smoothers, both Jacobi and symmetric Gauss-Seidel smoothers, satisfy the equivalence (3.4) (see [14, (5.1)]). This can be obtained by the property of the basis function. Taking the Jacobi smoother for an example, we have

$$(R_l^{-1} \widetilde{\phi}_l^p, \widetilde{\phi}_l^q)_{0,\rho} = \begin{cases} a_l(\widetilde{\phi}_l^p, \widetilde{\phi}_l^q), & p = q \in \mathcal{S}_l, \\ 0, & p, q \in \mathcal{S}_l \text{ and } p \neq q. \end{cases} \tag{3.5}$$

Then, for any $v = \sum_{p \in \mathcal{S}_l} v^p \widetilde{\phi}_l^p \in \widetilde{V}_l$, it holds that

$$\begin{aligned} (R_l^{-1} v, v)_{0,\rho} &= \sum_{p,q \in \mathcal{S}_l} (R_l^{-1} v^p \widetilde{\phi}_l^p, v^q \widetilde{\phi}_l^q)_{0,\rho} = \sum_{p \in \mathcal{S}_l} a_l(v^p \widetilde{\phi}_l^p, v^p \widetilde{\phi}_l^p) \\ &\simeq \sum_{p \in \mathcal{S}_l} (h_l^{-2} v^p \widetilde{\phi}_l^p, v^p \widetilde{\phi}_l^p)_{0,\rho} \simeq (h_l^{-2} v, v)_{0,\rho}, \end{aligned}$$

where in the third equality we have used $(\nabla\widetilde{\phi}_l^p, \nabla\widetilde{\phi}_l^p)_{0,\rho,\tau} \simeq (h_\tau^{-2}\widetilde{\phi}_l^p, \widetilde{\phi}_l^p)_{0,\rho,\tau}$ on each τ.

Let $\tilde{A}_l : \widetilde{V}_l \to \widetilde{V}_l$ $(1 \le l \le L)$ be the operator induced by $a_l(\cdot,\cdot)$ on $\widetilde{V}_l$, i.e.,

$$(\tilde{A}_l w, v)_{0,\rho} = a_l(w, v), \quad \forall w, v \in \widetilde{V}_l,$$

and P_l, $P_l^0 : V_L \to \widetilde{V}_l (1 \le l \le L)$ be defined by

$$a_l(P_l w, v) = a_L(u, I_l v), \quad (P_l^0 w, v)_{0,\rho} = (u, I_l v)_{0,\rho}, \quad \forall w \in V_L,\ v \in \widetilde{V}_l.$$

It follows from the above definitions that $\tilde{A}_l P_l = P_l^0 A_L$, where A_L is the operator induced by $a_L(\cdot,\cdot)$ on V_L.

Then the local multilevel preconditioner B_L for the mortar finite element method can be stated as

$$B_L = \sum_{l=1}^{L} I_l R_l \tilde{A}_l P_l A_L^{-1} = \sum_{l=1}^{L} I_l R_l P_l^0. \tag{3.6}$$

Remark 3.2. Here, we only introduce the local additive multilevel preconditioner. If we choose a suitable parameter μ_l, such that there exists ω_l $(0 < \omega_l < 2)$, which is independent of the jump in the coefficient, the mesh size and the mesh level, satisfying the stability of the local smoother:

$$a_L(I_l v_l, I_l v_l) \le \omega_l (\mu_l R_l^{-1} v_l, v_l)_{0,\rho}, \quad \forall v \in V_l,$$

we may also define an efficient local multiplicative multilevel preconditioner.

4. Analysis

In this section, we shall estimate the condition number of the preconditioned system. The following Poincaré type inequality (see [16, Theorem 3.1.1] or [24, Theroem 2.7.1]) is needed in the analysis.

Lemma 4.1. *Let L be a segment, μ be a piecewise linear function with non-vanishing average over L, then it holds for any v in $H^1(L)$ that*

$$\|v\|_{0,L} \lesssim C_\mu h_L \|\nabla v\|_{0,L} + \frac{1}{\left|\int_L \mu d\sigma\right|} \left|\int_L \mu v d\sigma\right|, \tag{4.1}$$

where $C_\mu = \frac{\int_L |\mu| d\sigma}{|\int_L \mu d\sigma|}$.

Proof. By density, it suffices to consider $v \in C^\infty(L) \cap H^1(L)$. The triangle inequality and the fundamental theorem of calculus yield

$$\begin{aligned}
\int_L v^2 d\sigma &\le 2\int_L \left(v - \frac{\int_L \mu v ds}{\int_L \mu ds}\right)^2 d\sigma + 2\int_L \left(\frac{\int_L \mu v ds}{\int_L \mu ds}\right)^2 d\sigma \\
&\le 2\frac{1}{\left(\int_L \mu ds\right)^2} \int_L \left(\int_L \mu (v(\sigma) - v(s)) ds\right)^2 d\sigma + 2\frac{h_L}{\left(\int_L \mu d\sigma\right)^2} \left(\int_L \mu v d\sigma\right)^2 \\
&\le 2\left(\frac{\int_L |\mu| ds}{\int_L \mu ds}\right)^2 h_L \left(\int_L |\nabla v| d\sigma\right)^2 + 2\frac{h_L}{\left(\int_L \mu d\sigma\right)^2} \left(\int_L \mu v d\sigma\right)^2 \\
&\lesssim C_\mu^2 h_L^2 \int_L |\nabla v|^2 d\sigma + \frac{1}{\left(\int_L \mu d\sigma\right)^2} \left(\int_L \mu v d\sigma\right)^2.
\end{aligned}$$

This completes the proof of the lemma. □

We show that the intergrid transfer operator is stable under the weighted L^2 norm and the energy norm.

Lemma 4.2. *For any $v \in V_l$, the following inequalities hold:*

$$\|I_l v\|_{0,\rho} \lesssim \|v\|_{0,\rho}, \tag{4.2}$$

$$\|I_l v\|_{a_{l+1}} \lesssim \|v\|_{a_l}. \tag{4.3}$$

Proof. By the definition of I_l, we note that $I_l v \neq v$ only on the element $\tau \in \mathcal{T}_{l+1}(\Omega)$ whose boundary has nonempty intersection with the nonmortar side. We just need to discuss the stability on these elements.

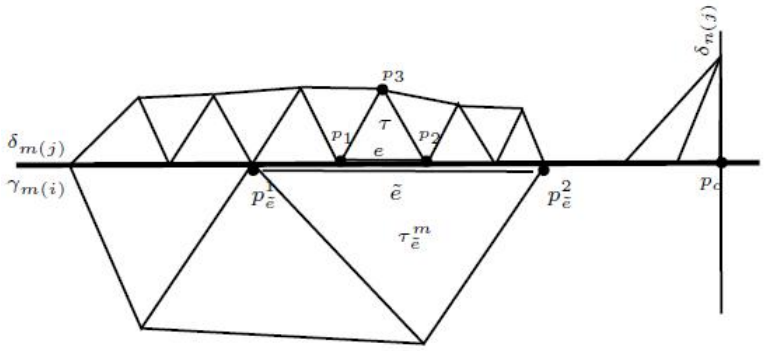

Fig. 4.1. Elements associated with the nonmortar and mortar sides.

The intersection of the boundary of τ and the nonmortar side may be an edge, a node, two edges, or an edge and its opposite node (see Fig. 4.1 for an illustration). If the intersection is the edge denoted by e, i.e., $\partial\tau \cap \bar{\delta} = \bar{e} = \overline{p_1 p_2}$, we denote p_3 the vertex opposite to e, $\tilde{e} = \overline{p_{\tilde{e}}^1 p_{\tilde{e}}^2}$ the mortar side edge associated with e, and $\tau_{\tilde{e}}^m$ the mortar side element which takes $\tilde{e}$ as an edge.

It follows from the norm equivalence, the scaling argument and the definition of I_l that

$$\begin{aligned}\|I_l v\|_{0,\rho,\tau}^2 &\simeq \rho_\tau h_\tau^2 \sum_{k=1}^{3} (I_l v(p_k))^2 \\ &= \rho_\tau h_\tau^2 \Big((v^j(p_3))^2 + (I_l^i v(p_1))^2 + (I_l^i v(p_2))^2 \Big) \\ &\lesssim \|v\|_{0,\rho,\tau}^2 + \rho_\tau h_e^2 \big(v^i(p_{\tilde{e}}^1))^2 + (v^i(p_{\tilde{e}}^2))^2 \big), \end{aligned} \tag{4.4}$$

where $v^i = v|_{\Omega_i}$, $v^j = v|_{\Omega_j}$ associated with the corresponding mortar and nonmortar side subdomains Ω_i and Ω_j. For the other cases, we can obtain similar inequalities by the same arguments.

Consequently, summing (4.4) over all the nonmortar side elements associated with the mortar side edge $\tilde{e}$, we have

$$\begin{aligned}\sum_\tau \|I_l v\|_{0,\rho,\tau}^2 &\lesssim \sum_\tau \|v\|_{0,\rho,\tau}^2 + \sum_{e\subset\tilde{e}} \rho_{\tau_e^{nm}} h_e^2 \Big((v^i(p_{\tilde{e}}^1))^2 + (v^i(p_{\tilde{e}}^2))^2 \Big) \\ &\leq \sum_\tau \|v\|_{0,\rho,\tau}^2 + \rho_{\tau_{\tilde{e}}^m} h_{\tilde{e}}^2 \Big((v^i(p_{\tilde{e}}^1))^2 + (v^i(p_{\tilde{e}}^2))^2 \Big) \lesssim \sum_\tau \|v\|_{0,\rho,\tau}^2 + \|v\|_{0,\rho,\tau_{\tilde{e}}^m}^2, \end{aligned} \tag{4.5}$$

where τ_e^{nm} denotes the nonmortar side element taking e as an edge, and in the second inequality we have used the fact that the coefficient on the mortar side subdomain is larger than the one on the nonmortar side subdomain. Then the inequality (4.2) follows form (4.5).

For the inequality (4.3), similarly, as the proof of (4.2), we consider the case that the edge e is the intersection of the boundary of the element τ and the nonmortar side δ (see Fig. 4.1 for example). By the norm equivalence, the definition of I_l and the triangle inequality, we derive that

$$\begin{aligned}
\|\nabla I_l v\|_{0,\rho,\tau}^2 &\simeq \rho_\tau\Big((I_l v(p_1) - I_l v(p_2))^2 + (I_l v(p_3) - I_l v(p_1))^2 + (I_l v(p_3) - I_l v(p_2))^2\Big) \\
&= \rho_\tau\Big((v^i(p_1) - v^i(p_2))^2 + (v^j(p_3) - v^i(p_1))^2 + (v^j(p_3) - v^i(p_2))^2\Big) \\
&\lesssim \rho_\tau |\nabla v^i|_e^2 h_e^2 + \rho_\tau \sum_{k=1}^{2}\Big(v^j(p_k) - v^i(p_k)\Big)^2 + \sum_{m,k=1}^{3}\rho_\tau\Big(v^j(p_m) - v^j(p_k)\Big)^2 \\
&\lesssim \rho_\tau |\nabla v^i|_e^2 h_e^2 + \rho_\tau h_e^{-1}\|(v^j - v^i)\|_{0,e}^2 + \|\nabla v\|_{0,\rho,\tau}^2. \qquad (4.6)
\end{aligned}$$

Let s_e be the union of the edges in $\mathcal{T}_l(\delta_{m(j)})$ sharing at least one node with e, and $\psi_e \in M_l(\delta_{m(j)})$ be the Lagrange multiplier basis function associated with one of the endpoints of e. Then, by the mortar condition, we have

$$\int_{s_e}(v^j - v^i)\psi_e d\sigma = 0,$$

which, together with Poincaré type inequality (4.1) ($C_\mu = \frac{5}{3}$), yields

$$h_e^{-1}\|(v^j - v^i)\|_{0,e}^2 \lesssim h_e(\|\nabla v^i\|_{0,s_e}^2 + \|\nabla v^j\|_{0,s_e}^2).$$

Consequently, we get

$$\begin{aligned}
\|\nabla I_l v\|_{0,\rho,\tau}^2 &\lesssim \rho_e h_e(\|\nabla v^i\|_{0,s_e}^2 + \|\nabla v^j\|_{0,s_e}^2) + \|\nabla v\|_{0,\rho,\tau}^2 \\
&\lesssim \|\nabla v\|_{0,\rho,\tau}^2 + \frac{h_e^2}{h_{\tilde{e}}^2}\|\nabla v\|_{0,\rho,\tau_{\tilde{e}}^m}^2 \\
&\le \|\nabla v\|_{0,\rho,\tau}^2 + \frac{h_e}{h_{\tilde{e}}}\|\nabla v\|_{0,\rho,\tau_{\tilde{e}}^m}^2. \qquad (4.7)
\end{aligned}$$

Here, we have used the fact that ∇v^j and ∇v^i are piecewise constants. For other nonmortar side elements, we can obtain (4.7) similarly. The proof of (4.3) is completed by summing (4.7) over all the nonmortar side elements τ. □

To get a stable space decomposition, we introduce a quasi-interpolation from the finest space V_L to the coarser space V_l. Let Π_l^i be the Scott-Zhang [20] interpolation operator defined on $\mathcal{T}_l(\Omega_i)$:

$$\Pi_l^i v = \sum_{p\in\mathcal{N}_l(\overline{\Omega}_i)}\int_{\sigma_p^l}\varphi_l^p v dx \phi_l^p, \quad \forall v \in H^1(\Omega_i), \qquad (4.8)$$

where ϕ_l^p and φ_l^p denote the P_1 basis function and its dual associated with the node p, σ_l^p is an edge of $\mathcal{T}_l(\Omega_i)$ defined as follows (see [10, 27]):

1. If the node $p \in \mathcal{N}_l(\overline{\Omega}_i) \cap \mathcal{N}_{l-1}(\overline{\Omega}_i)$ $(l > 1)$ satisfying $\phi_l^p = \phi_{l-1}^p$, we choose the edge $\sigma_l^p = \sigma_{l-1}^p$;
2. If p is other node in $\mathcal{N}_l(\overline{\Omega}_i)$, σ_l^p is an edge with one endpoint at p.

By the definition of Π_l^i, we introduce an operator $\Pi_l : V_L \to W_l \subset V_l$ as follows.

$$(\Pi_l v)(p) = \begin{cases} \left(\Pi_l^i v\right)(p), & \text{if } p \in \mathcal{N}_l(\Omega_i) \cup \mathcal{N}_l(\gamma_{m(i)}) \cup \mathcal{N}_l(\delta_{m(j)}), \\ v(p), & \text{if } p \in \mathcal{C}. \end{cases} \tag{4.9}$$

Lemma 4.3. *For any $v \in V_L$, we have the following approximations*

$$\|h_l^{-1}(v - \Pi_l v)\|_{0,\rho}^2 \lesssim \max_{e \in \mathcal{T}_l(\gamma)} \left(\frac{N_l^e}{J_e^\rho}, |\log h_{\min}^c| \right) \|v\|_{a_L}^2, \tag{4.10}$$

$$\|v - \Pi_l v\|_{a_L}^2 \lesssim \max_{e \in \mathcal{T}_l(\gamma)} \left(\frac{N_l^e}{J_e^\rho}, |\log h_{\min}^c| \right) \|v\|_{a_L}^2, \tag{4.11}$$

where $h_{\min}^c$ denotes the minimum size of elements around the cross points.

Proof. We only give the proof for the first inequality, and it is similar for the second one.

We note that Π_l is just the standard Scott-Zhang operator when restricted to the element $\tau \in \mathcal{T}_l(\Omega)$ satisfying $\partial\tau \cap (\delta \cup \mathcal{C}) = \emptyset$, and it holds for these elements that ([20])

$$\|h_l^{-1}(v - \Pi_l v)\|_{0,\rho,\tau} \lesssim |v|_{1,\rho,\omega_\tau}. \tag{4.12}$$

Here ω_τ denotes the union of the elements in the same subdomain which share at least a node with τ.

If there is an edge e of τ on the nonmortar side $\delta_{m(j)}$ (see Fig. 4.1), by the triangle inequality, the norm equivalence and the definition of Π_l, we deduce that

$$\begin{aligned} \|h_l^{-1}(v - \Pi_l v)\|_{0,\rho,\tau}^2 &\lesssim \|h_l^{-1}(v - \Pi_l^j v)\|_{0,\rho,\tau}^2 + \|h_l^{-1}(\Pi_l^j v - \Pi_l v)\|_{0,\rho,\tau} \\ &\lesssim |v|_{1,\rho,\omega_\tau}^2 + \rho_\tau \sum_{k=1}^{2} \left(\Pi_l^j v(p_k) - \Pi_l v(p_k) \right)^2. \end{aligned} \tag{4.13}$$

We next estimate the second term of (4.13). If $p_k \in \mathcal{N}_l(\delta_{m(j)})$ is a nonmortar side node, it holds for the corresponding Lagrange multiplier basis function $\psi_{m(j)}^{p_k} \in M_l(\delta_{m(j)})$ that

$$\bar{v}_{p_k} \triangleq \int_{s_{p_k}} v^j \psi_{m(j)}^{p_k} ds = \int_{s_{p_k}} v^i \psi_{m(j)}^{p_k} ds, \tag{4.14}$$

where s_{p_k} is the union of the edges in $\mathcal{T}_l(\delta_{m(j)})$ sharing p_k as an endpoint. Using the Schwarz inequality, the scaling argument, and the Poincaré type inequality (4.1), we have

$$\begin{aligned} (\Pi_l^j v(p_k) - \Pi_l v(p_k))^2 &\lesssim (\Pi_l^j v(p_k) - \bar{v}_{p_k})^2 + (\bar{v}_{p_k} - \Pi_l^i v(p_k))^2 \\ &\lesssim \left(\Pi_l^j v(p_k) - \bar{v}_{p_k} \right)^2 + \sum_{s=1}^{2} \left((\bar{v}_{p_k} - \Pi_l^i v(p_{\tilde{e}}^s) \right)^2 \\ &\lesssim h_\tau^{-2} \|\Pi_l^j v - \bar{v}_{p_k}\|_{0,\tau}^2 + h_{\tilde{e}}^{-2} \|\bar{v}_{p_k} - \Pi_l^i v\|_{0,\tau_{\tilde{e}}^m}^2 \\ &= h_\tau^{-2} \|\Pi_l^j (v - \bar{v}_{p_k})\|_{0,\tau}^2 + h_{\tilde{e}}^{-2} \|\Pi_l^i (\bar{v}_{p_k} - v)\|_{0,\tau_{\tilde{e}}^m}^2 \\ &\lesssim \|\nabla v\|_{0,\omega_\tau}^2 + \|\nabla v\|_{0,\omega_{\tau_{\tilde{e}}^m}}^2, \end{aligned} \tag{4.15}$$

where $p_{\tilde{e}}^s$, $s = 1, 2$, are the endpoints of the mortar side edge $\tilde{e}$ associated with e.

If $p_k \in \mathcal{C}$ is a cross point, $\bar{v} := \frac{1}{|\tau|}\int_\tau v ds$, by the triangle inequality, the Sobolev inequality (see [24, Lemma 10.1.1]), the Poincaré inequality and the scaling argument, we obtain

$$\begin{aligned}\left((\Pi_l^j v - \Pi_l v)(p_k)\right)^2 &\lesssim \left((\Pi_l^j v(p_c) - \bar{v}\right)^2 + \left((\bar{v} - v(p_k))\right)^2 \\ &\lesssim h_\tau^{-2}\|\Pi_l^j v - \bar{v}\|_{0,\tau}^2 + \|\bar{v} - v\|_{\infty,\tau}^2 \\ &\lesssim \|\nabla v\|_{0,\omega_\tau}^2 + |\log h_{\min}^c|\|\nabla v\|_{0,\tau}^2. \end{aligned} \tag{4.16}$$

Then, the inequality (4.10) follows from (4.12), (4.15) and (4.16). □

Lemma 4.4. *For any $v \in V_L$, there exists one decomposition of v*

$$v = \sum_{l=1}^{L} I_l v_l,\ v_l \in \widetilde{V}_l, \tag{4.17}$$

satisfying

$$\|v_1\|_{a_1}^2 + \sum_{l=2}^{L}(R_l^{-1}v_l, v_l)_{0,\rho} \lesssim \Lambda\|v\|_{a_L}^2, \tag{4.18}$$

where $\Lambda = \max\limits_{e\in\cup_l\mathcal{T}_l(\gamma)}\left(\frac{N_l^e}{J_e^p}, |\log h_{min}^c|\right)$.

Proof. For any $v \in V_L$, we choose a decomposition satisfying $v_L = v - \Pi_{L-1}v \in V_L$, $v_l = (\Pi_l - \Pi_{l-1})v \in W_l, 2 \le l \le L-1$, $v_1 = \Pi_1 v \in W_1$. Since $W_l \subset W_L \subset V_L$, it is true that

$$v = \sum_{l=1}^{L} v_l = \sum_{l=1}^{L} I_l v_l. \tag{4.19}$$

By the definition of Π_l, we have

$$\begin{aligned}&(\Pi_l v)(p) = (\Pi_{l-1}v)(p), \qquad \forall p \in \widetilde{\mathcal{N}}_l \setminus \mathcal{S}_l,\ 2 \le l < L,\\ &(\Pi_{L-1}v)(p) = v(p), \qquad \forall p \in \widetilde{\mathcal{N}}_L \setminus \mathcal{S}_L.\end{aligned}$$

Consequently, $v_l \in \widetilde{V}_l$ and the decomposition (4.17) is true.

Next we show that the decomposition is stable with the constant Λ. By (3.4), we have

$$(R_l^{-1}v_l, v_l)_{0,\rho} \simeq \sum_{p\in\mathcal{S}_l}\|h_l^{-1}v_l^p\|_{0,\rho}^2, \tag{4.20}$$

where $v_l^p = ((\Pi_l - \Pi_{l-1})v)(p)\widetilde{\phi}_l^p$, $1 < l < L$, and $v_L^p = (v - \Pi_{L-1}v)(p)\widetilde{\phi}_L^p$.

If $p \in \mathcal{S}_l \setminus (\mathcal{N}_l(\gamma) \cap \mathcal{C})$ is the node in Ω_i on which the smoother is performed, it follows from directly calculations that

$$\begin{aligned}\|h_l^{-1}v_l^p\|_{0,\rho}^2 &= |((\Pi_l - \Pi_{l-1})v)(p)|^2\|(h_l^{-1}\rho)^{\frac{1}{2}}\widetilde{\phi}_l^p\|_{0,\omega_p}^2 \\ &\simeq \rho_{\omega_p}|((\Pi_l - \Pi_{l-1})v)(p)|^2,\end{aligned} \tag{4.21}$$

where ω_p is the union of the elements in $\mathcal{T}_l(\Omega_i)$ sharing p as a vertex.

If $p \in \mathcal{S}_l \cap \mathcal{N}_l(\gamma)$ is one of the mortar side nodes on which the smoother is carried out, Ω_i and Ω_j are the mortar and nonmortar side subdomains associated with p, then,

$$\begin{aligned}\|h_l^{-1}v_l^p\|_{0,\rho}^2 &= |\left((\Pi_l-\Pi_{l-1})v\right)(p)|^2\int_\Omega \rho h_l^{-2}|\widetilde{\phi}_l^p|^2dx\\ &= |\left((\Pi_l-\Pi_{l-1})v\right)(p)|^2\left(\rho_p^m\int_{\Omega_i}h_l^{-2}|\widetilde{\phi}_l^p|^2dx+\rho_p^{nm}\int_{\Omega_j}h_l^{-2}|\widetilde{\phi}_l^p|^2dx\right)\\ &\lesssim |\left((\Pi_l-\Pi_{l-1})v\right)(p)|^2(\rho_p^m+\rho_p^{nm}n_p^{nm}).\end{aligned} \tag{4.22}$$

Here ρ_p^m and ρ_p^{nm} denote the coefficients on the mortar and nonmortar side subdomains associated with p, and n_p^{nm} indicates the number of the corresponding nonmortar side edges.

If $p \in \mathcal{S}_l \cap \mathcal{C}$ is a cross point, we note that $\left((\Pi_l-\Pi_{l-1})v\right)(p)$ vanishes by the definition of Π_l. Then it follows from the inequalities (4.20)-(4.22) that

$$\begin{aligned}&\sum_{l=2}^{L-1}(R_l^{-1}v_l,v_l)_{0,\rho}\\ &=\sum_{l=2}^{L-1}\left(\sum_{p\in\mathcal{S}_l\setminus\mathcal{N}_l(\gamma)}\|h_l^{-1}v_l^p\|_{0,\rho}^2+\sum_{p\in\mathcal{S}_l\cap\mathcal{N}_l(\gamma)}\|h_l^{-1}v_l^p\|_{0,\rho}^2\right)\\ &\lesssim\sum_{l=2}^{L-1}\sum_{p\in\mathcal{S}_l\setminus\mathcal{N}_l(\gamma)}\rho_{\omega_p}|\left((\Pi_l-\Pi_{l-1})v\right)(p)|^2\\ &\qquad+\sum_{l=2}^{L-1}\sum_{p\in\mathcal{S}_l\cap\mathcal{N}_l(\gamma)}\left(\rho_p^m(1+n_p^{nm}\frac{\rho_p^{nm}}{\rho_p^m})|\left((\Pi_l-\Pi_{l-1})v\right)(p)|^2\right)\\ &\le\max_{e\in\cup_l\mathcal{T}_l(\gamma)}\left(1+\frac{N_l^e}{J_e^\rho}\right)\sum_{i=1}^N\rho_{\Omega_i}\sum_{l=2}^{L-1}\sum_{p\in\mathcal{S}_l\cap\mathcal{N}_l(\overline{\Omega}_i)}|\left((\Pi_l^i-\Pi_{l-1}^i)v\right)(p)|^2.\end{aligned} \tag{4.23}$$

On each subdomain Ω_i, using the standard stability of space decomposition on local multilevel methods for the P_1 conforming element method (see, e.g., Theorem 3.5 in [10]), we have

$$\sum_{l=2}^{L-1}\sum_{p\in\mathcal{S}_l\cap\mathcal{N}_l(\overline{\Omega}_i)}|\left((\Pi_l^i-\Pi_{l-1}^i)v\right)(p)|^2\lesssim\|\nabla v\|_{0,\Omega_i}^2, \tag{4.24}$$

and consequently obtain

$$\sum_{l=2}^{L-1}(R_l^{-1}v_l,v_l)_{0,\rho}\lesssim\max_{e\in\cup_l\mathcal{T}_l(\gamma)}\left(1+\frac{N_l^e}{J_e^\rho}\right)\|v\|_{a_L}^2, \tag{4.25}$$

which, together with Lemma 4.3 and the definition of R_1, yields (4.18). □

Lemma 4.5. *We have the following global strengthened Cauchy-Schwarz inequality*

$$\sum_{l=1}^{L}\sum_{k=1}^{l-1}a_L(I_lv_l,I_kw_k)\lesssim\left(\sum_{l=1}^{L}\|I_lv_l\|_{a_l}^2\right)^{\frac{1}{2}}\left(\sum_{k=1}^{L}\|I_kw_k\|_{a_k}^2\right)^{\frac{1}{2}},\quad\forall v_l\in\widetilde{V}_l,\ w_k\in\widetilde{V}_k. \tag{4.26}$$

Proof. The main idea of the proof is to classify the elements according to the mesh size, and to use the technique of the strengthened Cauchy-Schwarz inequality on uniform grid.

For each element $\tau \in \mathcal{T}_l(\Omega)$, let $g(\tau)$ be the refined times of τ from $T_1 \in \mathcal{T}_1(\Omega)$. It is reasonable to assume that there exists θ, $0 < \theta < 1$, which only depends on the shape regularity of the mesh, satisfying ([13])

$$h_{T_1}\theta^{g(\tau)} \lesssim h_\tau \lesssim h_{T_1}\theta^{g(\tau)}. \tag{4.27}$$

Let $\mathcal{N}_l(\tau) \subset \widetilde{\mathcal{N}}_l$ be the set of the free nodes associated with τ, i.e., $\mathcal{N}_l(\tau) = \{p \in \widetilde{\mathcal{N}}_l, \tau \subset \mathrm{supp}\widetilde{\phi}_l^p\}$ (see Fig. 4.2 for an illustration). We note that $v_l \in \widetilde{V}_l$ can be rewritten as the summation of the functions associated with each node in $\mathcal{S}_l$, i.e., $v_l = \sum_{p\in\mathcal{S}_l} v_l^p$, $v_l^p \in \mathrm{span}\ \{\widetilde{\phi}_l^p\}$. v_l can also be rewritten as the summation of the functions corresponding to the refined times, that is

$$v_l = \sum_{m=0}^{\infty} \sum_{\substack{\tau\in\mathcal{T}_l(\Omega)\setminus\mathcal{T}_{l-1}(\Omega)\\ g(\tau)=m}} \sum_{p\in\mathcal{N}_l(\tau)} \tilde{v}_l^p,$$

where

$$\tilde{v}_l^p = \begin{cases} v_l^p/N_l(p), & \text{if } p \in \mathcal{S}_l, \\ 0, & \text{else,} \end{cases}$$

with $N_l(p)$ the number of the elements in $\mathcal{T}_l(\Omega) \setminus \mathcal{T}_{l-1}(\Omega)$ and the support of $\widetilde{\phi}_p^l$.

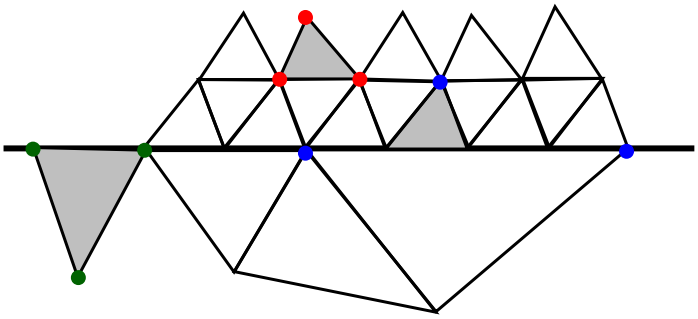

Fig. 4.2. An illustration of $\mathcal{N}(\tau)$.

Similarly, we rewrite w_k as

$$w_k = \sum_{n=0}^{\infty} \sum_{\substack{\kappa\in\mathcal{T}_k(\Omega)\setminus\mathcal{T}_{k-1}(\Omega)\\ g(\kappa)=n}} \sum_{q\in\mathcal{N}_k(\kappa)} \tilde{w}_k^q.$$

Without loss of generality, we assume $m \le n$. Let

$$\widetilde{w}_n = \sum_{k=1}^{l-1} \sum_{\substack{\kappa\in\mathcal{T}_k(\Omega)\setminus\mathcal{T}_{k-1}(\Omega)\\ g(\kappa)=n}} \sum_{q\in\mathcal{N}_k(\kappa)} I_k\tilde{w}_k^q.$$

For each $p \in \mathcal{N}_l(\tau) \cap \mathcal{N}_l(\bar{\Omega}_i)$ with $\tau \in \mathcal{T}_l(\Omega_i) \setminus \mathcal{T}_{l-1}(\Omega_i)$ and $g(\tau) = m$, using (3.2.16) in [10], we have

$$\int_{\Omega_i} \nabla(I_l\tilde{v}_l^p)\cdot\nabla\widetilde{w}_n dx$$

$$\lesssim \theta^{\frac{n-m}{2}}\|\nabla I_l\tilde{v}_l^p\|_{0,\omega_{l,i}^p}\left(\sum_{k=1}^{l-1}\sum_{\substack{\kappa\in\mathcal{T}_k(\Omega_i)\setminus\mathcal{T}_{k-1}(\Omega_i)\\ g(\kappa)=n}}\sum_{q\in\mathcal{N}_k(\kappa)\cap\mathcal{N}_k(\bar{\Omega}_i)}\|\nabla I_k\tilde{w}_k^q\|^2_{0,\omega_{k,i}^q}\right)^{\frac{1}{2}}, \tag{4.28}$$

with $\omega_{l,i}^p=\mathrm{supp}(I_l\tilde{v}_l^p)\cap\Omega_i$ and $\omega_{k,i}^q=\mathrm{supp}(I_k\tilde{w}_k^q)\cap\Omega_i$. It is derived by multiplying ρ both sides of the above inequality and summing over all Ω_i that

$$a_L(I_l v_l^p,\widetilde{w}_n)$$

$$\lesssim \theta^{\frac{n-m}{2}}\|\nabla I_l v_l^p\|_{0,\rho,\omega_l^p}\left(\sum_{k=1}^{l-1}\sum_{\substack{\kappa\in\mathcal{T}_k(\Omega)\setminus\mathcal{T}_{k-1}(\Omega))\\ g(\kappa)=n}}\sum_{q\in\mathcal{N}_k(\kappa)}\|\nabla I_k\tilde{w}_k^q\|^2_{0,\rho,\omega_k^q}\right)^{\frac{1}{2}}, \tag{4.29}$$

where $\omega_l^p=\mathrm{supp}(I_l\tilde{v}_l^p)$ and $\omega_k^q=\mathrm{supp}(I_k\tilde{w}_k^q)$. Then the proof is completed by summing (4.29) over all p in $\mathcal{N}_l(\tau)$, τ, and the refined times m, and using the fact that the spectral radius of $\{\theta^{|m-n|/2}\}_{m,n}$ is bounded. □

By the stable decomposition Lemma 4.4, the strengthened Cauchy-Schwarz inequality (4.26), and using the classical Schwarz framework, we have the following bound of the condition number of the preconditioned system.

Theorem 4.1. *For any $v\in V_L$, the inequalities*

$$(A_Lv,v)_{0,\rho}\lesssim(B_L^{-1}v,v)_{0,\rho},\ (B_L^{-1}v,v)_{0,\rho}\lesssim\Lambda(A_Lv,v)_{0,\rho} \tag{4.30}$$

are true, consequently, the condition number of the preconditioned system B_LA_L can be bounded as

$$\kappa(B_LA_L)\lesssim\Lambda, \tag{4.31}$$

where Λ is the parameter defined in (4.18).

Proof. Our proof is based on the following equivalence (see Lemma 2.5 in [21]):

$$(B_L^{-1}v,v)_{0,\rho}=\inf_{\substack{v_l\in\widetilde{V}_l\\ v=\sum_{l=1}^L I_lv_l}}\left(\|v_1\|_{a_1}^2+\sum_{l=2}^L(R_l^{-1}v_l,v_l)_{0,\rho}\right). \tag{4.32}$$

The second inequality of (4.30) follows from (4.32) and (4.18). We next prove the first inequality of (4.30). For any decomposition $v=\sum_{l=1}^L I_lv_l$, $v_l\in\widetilde{V}_l$, by Lemma 4.5, the inverse inequality, and the stability of I_l, we deduce that

$$\begin{aligned}a_L(v,v)&=\sum_{k,l=1}^L a_L(I_lv_l,I_kv_k)\le 2\sum_{l=1}^L\sum_{k=1}^l a_L(I_lv_l,I_kv_k)\\ &\lesssim\sum_{l=1}^L\|I_lv_l\|_{a_L}^2\lesssim\|I_1v_1\|_{a_L}^2+\sum_{l=2}^L\|h_l^{-1}I_lv_l\|_{0,\rho}^2\\ &\lesssim a_1(v_1,v_1)+\sum_{l=2}^L(h_l^{-2}v_l,v_l)_{0,\rho}\simeq a_1(v_1,v_1)+\sum_{l=2}^L(R_l^{-1}v_l,v_l)_{0,\rho}.\end{aligned} \tag{4.33}$$

Due to the arbitrariness of the decomposition and (4.32), we obtain

$$a_L(v,v) \lesssim \inf_{\substack{v_l \in \widetilde{V}_l \\ v=\sum_{l=1}^{L} I_l v_l}} \sum_{l=1}^{L} (R_l^{-1} v_l, v_l)_{0,\rho} = (B^{-1}v, v)_{0,\rho}. \tag{4.34}$$

5. Numerical Experiments

In this section we present a numerical result to illustrate the performance of our local multilevel preconditioner. The implementation is based on the FFW toolbox [6].

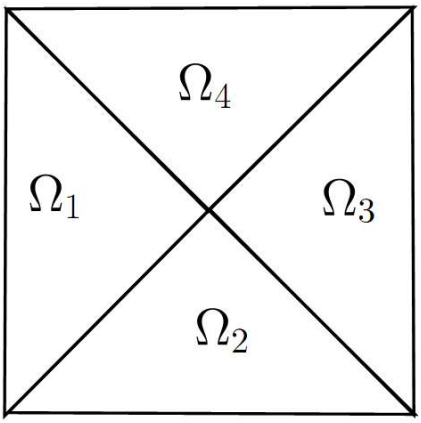

Fig. 5.1. The domain Ω.

The test problem is posed on the domain $\Omega = [0,1]^2$ with the piecewise constant coefficient. We choose the solution

$$u(x,y) = \frac{1}{\rho}(y-x)(1-x-y)(x-0.5)^2(y-0.5)^2,$$

with the corresponding right-hand side f and the Dirichlet boundary condition imposed on $\partial\Omega$, where ρ equals 1 on $\Omega_1 := \{(x,y) \in \Omega | x < y < 1-x\}$ and $\Omega_3 := \{(x,y) \in \Omega | y < x < 1-x\}$,

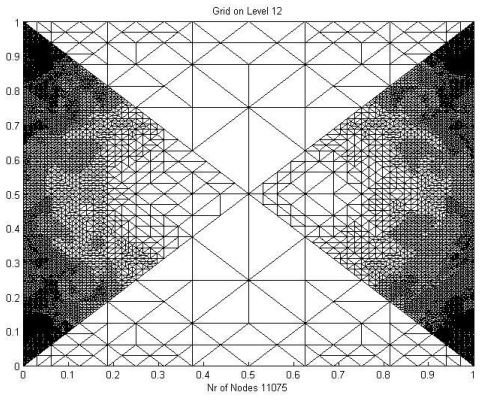

Fig. 5.2. The adaptive mesh after 12 refinements.

and takes different values $\rho = 10^i$ on $\Omega_2 := \{(x,y) \in \Omega | x > y > 1-x\}$ and $\Omega_4 := \{(x,y) \in \Omega | 1-y < x < y\}$ (see Fig. 5.1).

In the adaptive algorithm, we start with the initial triangulation $\mathcal{T}_1(\Omega) = \{\Omega_i\}$, and use the newest vertex bisection algorithm in each subdomain based on the error estimator introduced in [23]. We note that the mesh is not required to match across the subdomains interface. In Fig. 5.2, we draw the adaptive mesh after 12 refinements when the jump of the coefficient is 10^4.

Table 5.1: The iteration number and the condition number.

L	$i=2$	$i=4$	$i=6$	$i=8$
8	25(10.42)	23(10.62)	23 (10.61)	23 (10.62)
9	25(10.5)	24(10.73)	23 (10.57)	23(10.61)
10	26(10.48)	23(10.57)	24 (10.61)	23 (10.57)
11	26(10.5)	27(10.7)	29 (10.74)	24(10.61)
12	27(10.52)	27(10.69)	29 (10.74)	33(10.78)
13	27(10.57)	27(10.67)	29 (10.7)	30(10.76)
14	27(10.59)	24(10.56)	24 (10.56)	33 (10.79)
15	27(10.53)	28(10.7)	32 (10.79	33(10.8))
16	27(10.51)	28(10.63)	32 (10.78)	33(10.8)
17	27(10.48)	28(10.67)	32 (10.79)	25(10.55)
18	27(10.46)	28(10.65)	32 (10.79)	34(10.81)
19	29(10.49)	28(10.63)	32 (10.78)	33(10.8)
20	27(10.42)	30(10.69)	32 (10.77)	33(10.8)

For the local multilevel preconditioner, we use one symmetric Gauss-Seidel iteration as the smoother on each fine level, and the exact solver on the coarsest level. In Tables 5.1, we list the number of iterations, the condition numbers $\kappa(B_L A_L)$ with different jumps and mesh levels. From the table, we can see that the method is quite robust with respect to the jump in the coefficient, the mesh level, and the mesh size. This is consistent with our theoretical results.

Acknowledgments. The authors thank the referees and the editor for their helpful comments and suggestions. This work was supported by the National Science Foundation (NSF) of China (Grants No. 11071124, 11171335, 11226334, 11371199 and 11301275), the Program of Natural Science Research of Jiangsu Higher Education Institutions of China (Grant No. 12KJB110013), and the Doctoral fund of Ministry of Education of China (Grant No. 20123207120001).

References

[1] C. Bernardi, Y. Maday, A. Patera, Domain decomposition by the mortar element method, in Asymptotic and Numerical Methods for Partial Differential Equations with Critical Parameters, H.G. Kaper, M. Garbey, G. W. Pieper (ed.), Kluwer Academic Publishers, Dordrecht, 1993, 269-286.

[2] C. Bernardi, Y. Maday, A. Patera, A new nonconforming approach to domain decomposition: the mortar element method, in: Nonlinear Partial Differential Equations and their Application, H. Brezis, J. L. Lions (ed.), College de France Seminar, Vol. XI, Pitman, London, 1994, 13-51.

[3] C. Bernardi, R. Verfürth, Adaptive finite element methods for elliptic equations with nonsmooth coefficients, *Numer. Math.*, **85** (2000), 579-608.

[4] J. Bramble, J. Xu, Some estimates for a weighted L^2 projection, *Math. Comp.*, **56** (1991), 463-476.

[5] S. C. Brenner, Poincaré-Friedrichs inequalities for piecewise H_1 functions, *SIAM J. Numer. Anal.*, **41** (2003), 306-324.
[6] A. Byfut, J. Gedicke, D. Günther, J. Reininghaus, S. Wiedemann, *FFW documentation*, Humboldt University of Berlin, Germany, 2007.
[7] C. Carstensen, J. Hu, A unifying theory of a posteriori error control for nonconforming finite element methods, *Numer. Math.*, **107** (2007), 473-502.
[8] C. Carstensen, J. Hu, A. Orlando, Framework for the a posteriori error analysis of nonconforming finite elements, *SIAM J. Numer. Anal.*, **45** (2007), 62-82.
[9] C. Carstensen, J. Hu, Hanging nodes in the unifying theory of a posteriori finite element error contorl, *J. Comp. Math.*, **27** (2009), 215-236.
[10] H. Chen, Research on Local Multilevel Mehtods, PhD thesis, LSEC, AMSS, 2011.
[11] H. Chen, X. Xu, Local multilevel methods for adaptive finite element methods for nonsymmetric and indefinite elliptic boundary value problems, *SIAM J. Numer. Anal.*, **47** (2010), 4492-4516.
[12] H. Chen, X. Xu, W. Zheng, Local multilevel methods for second order elliptic problems with highly discontinuous coefficients, *J. Comp. Math.*, **30** (2012), 223-248.
[13] L. Chen, R. Nochetto, J. Xu, Optimal multilevel methods for graded bisection grids, *Numer. Math.*, **120**:1 (2011), 1-34.
[14] L. Chen, M. Holst, J. Xu, Y. Zhu, Local multilevel preconditioners for elliptic equations with jump coefficients on bisection grids, submitted, 2011.
[15] L. Chen, C.S. Zhang, A coarsening algorithm on adaptive grids by newest vertex bisection and its applications, *J. Comput. Math.*, **28**:6 (2010), 767-789.
[16] P.G. Ciarlet, The Finite Element Method for Elliptic Problems, North-Holland, Amsterdam, 1978.
[17] J. Gopalakrishnan, J.P. Pasciak, Multigrid for the mortar finite element method, *SIAM J. Numer. Anal.*, **37** (2000), 1029-1052.
[18] P. Lu, Z. Shi, X. Xu, Local multilevel methods for adaptive discontinuous Galerkin finite element methods (in Chinese), *Sci. China Math.*, **42** (2012), 409-428.
[19] W.F. Mitchell, Optimal multilevel iterative methods for adaptive grids, *SIAM J. Sci. Stat. Comput.*, **13** (1992), 146-167.
[20] L.R. Scott, S. Zhang, Finite-element interpolation of non-smooth functions satisfying boundary conditions, *Math. Comp.*, **54** (1990), 483-493.
[21] A. Toselli, O. Widlund, Domain Decomposition Methods: Algorithms and Theory, Springer-Verlag, Berlin, 2005.
[22] F. Wang, J. Chen, P. Huang, A multilevel preconditioner for the Crouzeix-Raviart finite element method for elliptic problems with discontinuous coefficients, *Sci. China Math.*, **55** (2012), 1513-1526.
[23] F. Wang, X. Xu, Some new residual-based a posteriori error estimators for the mortar finite element methods, *Numer. Math.*, **120** (2012), 543-571.
[24] L. Wang, X. Xu, The Mathematical Foundation the Finite Element Method, Science Press, Beijing, 2004.
[25] B.I. Wohlmuth, A mortar finite element method using dual spaces for the Lagrange multiplier, *SIAM J. Numer. Anal.*, **38** (2000), 989-1012.
[26] B.I. Wohlmuth, A V-cycle multigird approach for mortar finite elements, *SIAM J. Numer. Anal.*, **42** (2005), 2476-2495.
[27] H. Wu, Z. Chen, Uniform convergence of multigrid V-cycle on adaptively refined finite element meshes for second order elliptic problems, *Sci. China Math.*, **39** (2006), 1405-1429.
[28] J. Xu, Y. Zhu, Uniformly convergent multigrid methods for elliptic problems with strongly discontinuous coefficients, *Math. Mod. Meth. Appl. S.*, **18** (2008), 77-105.
[29] X. Xu, H. Chen, R. Hoppe, Optimality of local multilevel methods on adaptively refined meshes for elliptic boundary value problems, *J. Numer. Math.*, **18** (2010), 59-90.
[30] X. Xu, H. Chen, R. Hoppe, Optimality of local multilevel methods for adaptive nonconforming

P_1 finite element methods, *J. Comp. Math.*, **31** (2013), 22-46.

[31] X. Xu, J. Chen, Multigrid for the mortar element method for P_1 nonconforming element, *Numer. Math.*, **88** (2001), 381-398.